

Effect of ATPase Inhibitors on Cell Potential and K⁺ Influx in Corn Roots¹

Received for publication June 26, 1979 and in revised form February 11, 1980

JOHN M. CHEESEMAN, PETER R. LAFAYETTE, JOHN W. GRONWALD, AND JOHN B. HANSON
Department of Botany, University of Illinois, Urbana, Illinois 61801

ABSTRACT

Experiments were performed to determine the effect of plasmalemma ATPase inhibitors on cell potentials (ψ) and K⁺ (⁸⁶Rb) influx of corn root tissue over a wide range of K⁺ activity. *N,N'*-Dicyclohexylcarbodiimide (DCCD), oligomycin, and diethylstilbestrol (DES) pretreatment greatly reduced active K⁺ influx and depolarized ψ at low, but not at high, K⁺ activity (K^o). More comprehensive studies with DCCD and anoxia showed nearly complete inhibition of the active component of K⁺ influx over a wide range of K^o, with no effect on the apparent permeability constant. DCCD had no effect on the electrogenic component of the cell potential (ψ_p) above 0.2 millimolar K^o. Net proton efflux was rapidly reduced 80 to 90% by DCCD. Since tissue ATP content and respiration were only slightly affected by the DCCD-pretreatment, the inhibitions of active K⁺ influx and ψ_p at low K^o can be attributed to inhibition of the plasmalemma ATPase.

It is concluded that by DCCD treatment, the energy-linked electrogenic system at high K^o is separated from the energy-linked K⁺ influx system at low K^o. The results are analyzed in terms of electrical analogue models of the membrane. The presence of two, algebraically additive electrogenic components is indicated; one is better modeled as a current source (system I) and one as a voltage source (system II). No K⁺ stimulation of system II is required to produce the observed K^o dependence of ψ_p .

In previous papers we have examined the K⁺ dependence of the ψ^2 in 4-h washed corn roots (11) and the relationship of potential to K⁺ influx (12). The membrane potential had an electrogenic component which was strongly dependent in magnitude on K^o and which had a minimum in the range where $\psi \approx E_K$ (0.5–2 mM K^o) (11). This was the same range in which the passive contribution to K⁺ influx became noticeable (12).

In these experiments ψ_p and K⁺ influx were inhibited by cutting off the energy supply through uncoupling or anoxia. If a membrane ATPase is involved as we (12, 29, 30) and others (19, 23, 31, 33, 35, 36) have postulated, more direct evidence should be obtainable through the use of a plasmalemma ATPase inhibitor. Here, we report such experiments using DCCD, oligomycin, and DES, all of which have been suggested to produce this inhibition.

DCCD is a potent ATPase inhibitor in isolated mitochondria

(25), chloroplasts (25), and plasmalemma fractions from lower (6) and higher (5, 27) plants. In those cases where mode of action has been established, DCCD appears to block H⁺ transport by covalent binding to the oligomycin-sensitive subunit of the ATPase (25). In higher plants this results in reduced cell enlargement (34), H⁺ efflux (34) and K⁺ influx (10), physiological phenomena commonly associated with plasmalemma ATPase. However, DCCD is a potent chemical reagent which has the potential to react at other sites. At high concentrations, DCCD inhibits the basal activity of the (Na⁺ + K⁺)-activated ATPase (39). It has been noted to increase membrane permeability in *Chara* (23), to depolarize and cause loss of pH sensitivity of cell potential in darkened *Lemna* (31), to reduce the pH sensitivity of K⁺ influx in rat liver mitochondria (15), and to inhibit the H⁺ translocation associated with Cyt oxidase (9). Some caution is needed in interpreting DCCD responses as due to ATPase inhibition unless confirmed by other ATPase inhibitors.

Oligomycin, on the other hand, is highly specific for the ATPase proton channel of mitochondrial, bacterial, and chloroplast membranes (25). It is also effective in blocking energy-linked ion uptake by higher plant cells (2, 21). Although oligomycin does not inhibit the K⁺ stimulated, Mg²⁺-requiring ATPase of isolated plasmalemma fractions (27, 28) histochemical staining indicates that it blocks both plasmalemma and mitochondrial ATPases *in vivo* (32).

DES has been reported to be a much more effective inhibitor of the plasmalemma ATPase than of the mitochondrial ATPase (2). However, DES also inhibits oxidative phosphorylation (2). Severe membrane damage has been reported for both plant cells, in which DES causes rapid loss of previously acquired ⁸⁶Rb label (3), and mitochondria, in which DES caused solubilization of 25–30% of the mitochondrial protein and nearly complete release of bound Ca²⁺ and Mg²⁺ (8).

In the work reported here, we find that all three inhibitors effectively reduce K⁺ influx and electrical potential at low K^o (in the mechanism I range), but have smaller effects at higher K^o (in the mechanism II range). A detailed examination of the action of DCCD shows that while mechanism I is nearly completely inhibited, as evidenced by the reduction of net H⁺ efflux, active K⁺ influx, and ψ_p , the electrogenic system of mechanism II is DCCD insensitive. Possibilities as to the nature of mechanism II are discussed briefly.

Some of these data have been given in a preliminary report (10).

MATERIALS AND METHODS

Methods for raising corn seedlings [*Zea mays* L., (A619 × Oh43) × A632 Crow's Hybrid Corn Co., Milford, Ill.], cutting and washing root segments, and determination of cell potential, H⁺ efflux, and K⁺ influx were as previously described (11, 12, 17). Briefly, these are 0.5- to 2.5-cm segments of primary root which have been washed for 4 h at 30 C in 0.2 mM CaCl₂ + 0.2 mM Mes

¹ Supported by Grant PCM 76-80886 from the National Science Foundation and Contract EY 76-S-02-0790 from the United States Department of Energy.

² Abbreviations: ψ , ψ_D , and ψ_p : total, diffusion, and electrogenic components, respectively, of membrane potential; K^o, Kⁱ: external and internal K⁺ activity; E_K: Nernst potential for potassium; DCCD: *N,N'*-dicyclohexylcarbodiimide; DES: diethylstilbestrol; FCCP: *p*-fluoromethoxycarbonyl cyanide phenylhydrazone; P_i: permeability coefficient for ion *i*; ρ_i = P_i/P_K.

buffer adjusted to pH 6.0 with Tris. The medium for K^+ influx and ψ measurement was the same with variable additions of K_2SO_4 . Labeling was with ^{86}Rb (minimum of 20,000 cpm/ml, about 2 μM Rb), which is an effective tracer for K^+ influx in corn root tissue (22). For H^+ efflux studies, $CaSO_4$ was substituted for $CaCl_2$ and buffer was reduced to 60 μM . Concentration to activity corrections were based on Table 2.1 of reference 37.

Inhibitors were dissolved in ethanol and added to the solutions to give 50 μM DCCD, 1 $\mu g/ml$ oligomycin, or 20 μM DES. Final ethanol was 0.5%. Inhibitors were applied as a 30-min pretreatment in the washing solution; except for DES they were not present during experimental determinations. DES treatment was continued during K^+ influx determinations (10 min) in an attempt to reduce variability at low K^+ , but this was not very successful. Since all of these ATPase inhibitors can inhibit mitochondrial ATP production we selected concentrations and time of exposure which experience (29, 32; unpublished results) suggests will give 90% or greater inhibition of K^+ influx at low K^+ without significant effect on respiration or ATP levels. In the case of DCCD, which was selected for detailed study, this was checked (see under "Results").

For electrical and pH recordings, sections were pretreated as above except in experiments where the time course of inhibition was studied. In these experiments the inhibitors were added after baselines were established.

ATP analysis was as previously described (17). Respiration rates were determined using a Clark O_2 electrode (Yellow Springs Instruments).

RESULTS

Table I shows the effect of DCCD, oligomycin and DES on K^+ (^{86}Rb) influx and cortical cell potential at low and high K^+ . The inhibitors had similar effects, with DCCD reducing K^+ influx almost completely at low K^+ . On a percentage basis, reduction of K^+ influx was greater at low K^+ than at high K^+ . Effects on cell potentials were most pronounced at low K^+ . None of these inhibitors reduced ψ as much as anoxia or the uncoupler FCCP (12), and in all cases an inhibitor insensitive, anoxia sensitive component remained (see below).

In view of the reported adverse effects of DES on membrane integrity (see above and ref. 3) we looked for membrane leakage under our experimental conditions. One hour of treatment with 20 μM DES following a 10-min labeling period gave no increased loss of label over controls.

At $K^+ = 20 \mu M$ K^+ influx is active transport (12). Clearly the

ATPase inhibitors effectively block this system. At $K^+ = 4.6$ mM inhibition was only about two-thirds as great (Table I). Balke and Hodges (3) have reported DES to be less effective as K^+ increases. Previously (12) we have defined a parameter, η_K , such that passive influx of K^+ can be described,

$$\bar{\phi}_K = \eta_K K^+ \frac{\psi}{1 - \xi} \quad (1)$$

where $\bar{\phi}_K = K^+$ influx ($\mu mol/g$ fresh weight $\cdot h$), and $\xi = \exp(F\psi/RT)$. η_K is directly proportional to P_K but empirically allows for the unknown flux geometry and membrane surface area to weight ratio of the complex tissue. Under anoxia, K^+ influx was found to fit the relationship predicted with constant $\eta_K = 0.0059$ (12). In the experiments of Table I, using the values for $\bar{\phi}_K$ and ψ for inhibited tissue at $K^+ = 4.6$ mM, the values of η_K range from 0.0054 to 0.0062. Thus, the remaining K^+ influx at high K^+ is at a rate appropriate for passive flux. At $K^+ = 4.6$ mM, about one-third of the uptake is passive influx via mechanism II, while the inhibited two-thirds was by the active transport process of mechanism I (12). As ψ was not greatly reduced in the mechanism II range (Table I) and preliminary experiments showed an anoxia-sensitive component to remain, the data suggest the electrogenic system of the mechanism II range is not mediated by the affected plasmalemma ATPase. To further consider this we made more detailed studies at a wider range of K^+ , concentrating our efforts on the action of DCCD. To substantiate the view that the primary action was at the plasmalemma, we first established that 30-min treatment with 50 μM DCCD reduced cell ATP levels only slightly (from 117 ± 4 to 107 ± 4 nmol/g fresh weight) and had no statistically significant effect on O_2 uptake rates (15.1 and 14.1 $\mu mol O_2/g$ fresh weight $\cdot h$ at 24 C for control and DCCD treatment, respectively). Furthermore, no "salt respiration" was found on increasing K^+ from 0.2 mM to 14 mM with K_2SO_4 .

Figure 1 shows the K^+ dependence of ψ in control and DCCD treated tissues under aerobic and anoxic conditions. At $K^+ = 0.2$ mM, both total (ψ) and anoxic (ψ_D) potentials were unaffected by DCCD, both statistically and, in the case of ψ , in continuous single cell recordings over a 30-min treatment period. However, ψ was reduced both at lower and higher K^+ . Under anoxia, ψ_D was unaffected at low K^+ , but was reduced by DCCD at higher K^+ .

Based upon the linear ξ criterion (11) ψ under anoxia was a diffusion potential in both treated and untreated tissue. The ξ parameters are given in Table II. DCCD alters the apparent internal K^+ compartmentation, as indicated by the change in slope of the ξ plot, in a fashion similar to that previously suggested for FCCP; that is, K^+ as estimated from ξ is about that of the bulk

Table I. Effect of ATPase Inhibitors on K^+ (^{86}Rb) Influx and Cell Potential as a Function of External K^+ Activity

Flux units are $\mu mol/g$ fresh wt $\cdot h$. Potential units are mv. Means \pm SD shown. Numbers in parentheses refer to the number of determinations for flux values and number of determinations in number of roots for potentials.

| | $K^+ mM$ | | |
|----------------|-----------------------|-----------------------|-----------------------|
| | 0.02 | 0.2 | 4.6 |
| Control | | | |
| $\bar{\phi}_K$ | 3.5 ± 0.6 (16) | 4.5 ± 0.8 (7) | 6.9 ± 0.6 (16) |
| ψ | -142 ± 8 (11, 9) | -121 ± 5 (42, 24) | -100 ± 7 (22, 12) |
| DCCD | | | |
| $\bar{\phi}_K$ | 0.047 ± 0.001 (6) | 0.17 ± 0.006 (3) | 2.4 ± 0.2 (6) |
| ψ | -123 ± 7 (4, 3) | -113 ± 8 (10, 6) | |
| Oligomycin | | | |
| $\bar{\phi}_K$ | 0.39 ± 0.2 (14) | | 2.7 ± 0.2 (9) |
| ψ | -124 ± 8 (11, 7) | -117 ± 5 (42, 12) | -92 ± 7 (17, 9) |
| DES | | | |
| $\bar{\phi}_K$ | 0.27 ± 0.2 (14) | | 2.4 ± 0.5 (11) |
| ψ | -117 ± 6 (11, 6) | -107 ± 7 (30, 11) | -93 ± 5 (9, 4) |

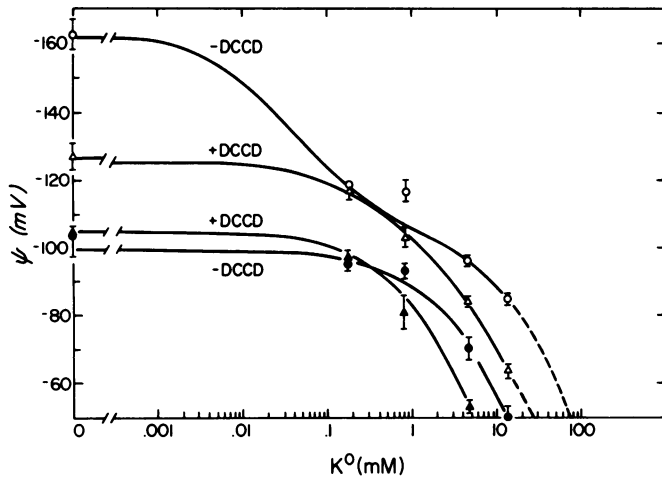


FIG. 1. K° dependence of ψ in control and DCCD-pretreated tissue. Open symbols, aerobic; closed symbols, anoxia. Means \pm SD shown. Curves were drawn from the ξ versus K° relationships by the equation given in Table II.

Table II. ξ Parameters for Control and DCCD-treated Roots under Aerobic and Anoxic Conditions

$$\psi = \frac{RT}{F} \ln \xi = \frac{RT}{F} \ln \left[\frac{K^{\circ} + A}{K^{\circ} + B} \right] (\alpha K^{\circ} + \beta)$$

(from ref. 11).

| | A ^a | B | α | β | K^i | $\rho_{Cl}Cl^i$ |
|----------------|----------------|--------|----------|---------|-----------------|-----------------|
| | | | | | mM ^a | mM ^b |
| Control | 0.0108 | 0.1090 | 0.00132 | 0.0135 | | |
| Anoxia | | | 0.0091 | 0.0222 | 110 | 2.4 |
| +DCCD | 0.1263 | 0.2630 | 0.0051 | 0.0150 | | |
| +DCCD + anoxia | | | 0.0249 | 0.0181 | 40 | 0.7 |

^a Calculated as the inverse of the slope of ξ versus K° .

^b Calculated as the x intercept of ξ versus K° .

tissue (12). There is also a reduction in $\rho_{Cl}Cl^i$, indicating DCCD must also alter ρ_{Cl} or Cl^i . As $\rho_{Cl}Cl^i$ and K^i are reduced proportionately, and as P_K is apparently unchanged (see below), it seems likely that Cl^i is the affected value. These results further emphasize that ψ_D is a function of the means used to reveal it (12). They do, however, demonstrate that an energy linked component of ψ exists even in the presence of ATPase inhibitors (Fig. 1).

Using anoxia as the standard for revealing ψ_D , the parameters of Table II were used to calculate ψ_p (11) for control and DCCD-treated roots (Fig. 2). At $K^{\circ} < 1$ mM, the electrogenic system is strongly inhibited by DCCD. The anoxia-induced depolarization is virtually unchanged at higher K° , though there is a slight shift in the K° at which ψ_p is minimal. This may be associated with the shift in the electrical crossover point (where $\psi = E_K$). For analysis, we will separate ψ_p into a DCCD-sensitive component (ψ_p^I) and a DCCD-insensitive component (ψ_p^{II}) such that

$$\psi_p = \psi_p^I + \psi_p^{II} \quad (2)$$

The justification for this algebraic relationship is discussed in the appendix.

The effectiveness of DCCD in reducing K^+ influx is shown in Table III. The effect on net H^+ efflux is shown in Table IV. The rapidity of DCCD action on proton efflux at $K^{\circ} = 0.2$ mM is shown in Figure 3. As noted above, under the same conditions ψ was unaffected in continuous recordings. When K^+ influx is

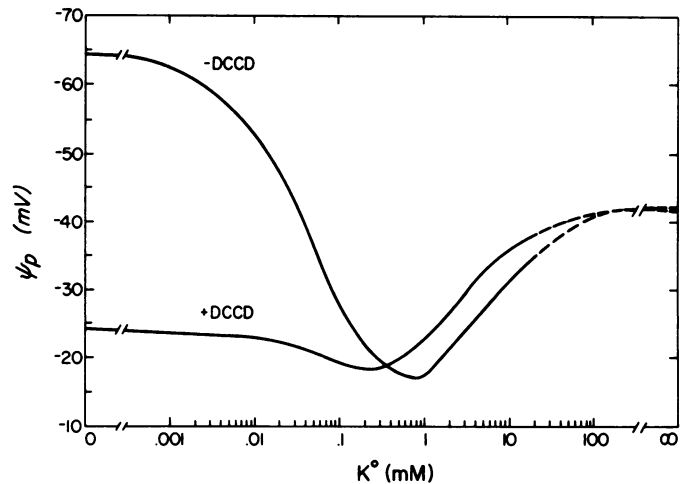


FIG. 2. K° dependence of ψ_p calculated from the parameters and equation in Table II. ψ_p represents the amount of depolarization caused by anoxia treatment. Details of the calculations were given in reference 11.

measured during the first 30 min of DCCD treatment, influx is reduced 81% at $K^{\circ} = 0.2$ mM, indicating that effect is also very rapid. The results of Table IV show that net H^+ efflux is less affected at high K° , as is K° influx. However, it is not possible to determine the actual H^+ efflux without detailed and presently unavailable knowledge of H^+ co-transport systems. Phosphate uptake, which probably proceeds via Pi^-/H^+ symport or Pi^-/OH^- antiport (29), is reduced by DCCD from 0.64 to 0.40 $\mu\text{mol/g}$ fresh weight \cdot h (38%), indicating other proton transporting systems are still functioning.

Agreement between actual K^+ influx and that predicted by the passive model (12) using the regression values of η_K given in Table III is shown in Figure 4, using a log-log plot to encompass the ranges. Where active flux is inhibited by DCCD and/or anoxia the fit is close, deviating by at most a factor of 3.7 in the DCCD treatment at the lowest value of K° . If η_K is indeed independent of K° , this must represent a very small remnant of active transport. Still, the reduction of active influx is greater than 98% under this worst case.

The similarity of the regression values of η_K (Table III) suggests that K^+ permeability is unaltered by any of the treatments. This differs from the effect of DCCD in *Chara*, for which Keifer and Spanswick (22) reported an increase in K^+ influx and while ψ was reduced, thus giving an apparent increase in P_K .

DISCUSSION

In these experiments we applied inhibitors of the plasmalemma ATPase and determined cell potential and K^+ influx over a wide range of K° . In the case of DCCD we showed the effects not to be due to a reduction of respiratory energy supply. Using anoxia, we determined the presence of an energy-linked K^+ influx and electrogenic potential in the presence of the blocked ATPase. In part, this might be due to imperfect inhibition of the plasmalemma ATPase by DCCD, at least in the deeper layers of the cortex (32), but the fact that the additional inhibition with anoxia was trivial at low K° compared to high K° (Table III, Figs. 1 and 2) indicates that there are two electrogenic systems in corn roots.

The first system, which we designate ψ_p^I , is active at low K° (mechanism I range), is sensitive to ATPase inhibitors, and is probably associated with active K^+ influx and H^+ efflux. The second, ψ_p^{II} , active at all K° levels becomes significant in the mechanism II range, drives passive cation influx and is insensitive to the ATPase inhibitors. Displacement of ψ from ψ_D is by the

Table III. K^+ (^{86}Rb) Influx to Control and DCCD-treated Root Segments under Aerobic and Anoxic Conditions
Control data previously reported (12). η_K values were determined by linear regression (see ref. 12).

| K° | -DCCD | | +DCCD | |
|-------------|---|-------------------------|------------------------|-------------------------|
| | Aerobic | Anoxic | Aerobic | Anoxic |
| <i>mM</i> | <i>$\mu\text{mol/g fresh wt} \cdot \text{h} \pm \text{SD}$</i> | | | |
| 0.002 | 0.42 \pm 0.1 (7) ^a | 0.0033 \pm 0.0005 (4) | 0.0058 \pm 0.003 (8) | 0.0023 \pm 0.0009 (4) |
| 0.002 | 2.5 \pm 0.8 (8) | 0.024 \pm 0.003 (4) | 0.047 \pm 0.01 (6) | 0.018 \pm 0.005 (4) |
| 0.2 | 4.6 \pm 0.4 (4) | 0.13 \pm 0.004 (3) | 0.16 \pm 0.01 (6) | 0.14 \pm 0.03 (4) |
| 4.6 | 6.8 \pm 0.6 (8) | 2.2 \pm 0.3 (3) | 2.4 \pm 0.2 (6) | 2.2 \pm 0.5 (4) |
| 13.8 | 10.7 \pm 1.3 (4) | 4.7 \pm 0.1 (3) | 5.2 \pm 0.9 (6) | 3.9 \pm 0.7 (4) |
| η_K | | 0.0059 | 0.0055 | 0.0069 |

^a Number of determinations.

Table IV. Effect of DCCD Pretreatment on Net H^+ Efflux, Determined by Back Titration after 30 Min

Medium contained 0.2 mM $CaCl_2$ and K-phosphate buffer (pH 6.0) for $K^{\circ} = 0.02$ and 0.2 mM. For $K^{\circ} = 4.6$ mM, medium contained 0.2 mM K-phosphate plus 2.9 mM K_2SO_4 .

| K° (mM) | H^+ Efflux | | |
|------------------|---|-------------------|--------------------|
| | 0.02 | 0.2 | 4.6 |
| | <i>$\mu\text{mol/g fresh wt} \cdot \text{h} \pm \text{SD}$</i> | | |
| -DCCD | 1.3 \pm 0.1 (3) ^a | 2.2 \pm 0.1 (3) | 2.2 \pm 0.1 (8) |
| +DCCD | 0.2 \pm 0.2 (3) | 0.2 \pm 0.1 (3) | 0.5 \pm 0.01 (3) |

^a Number of determinations.

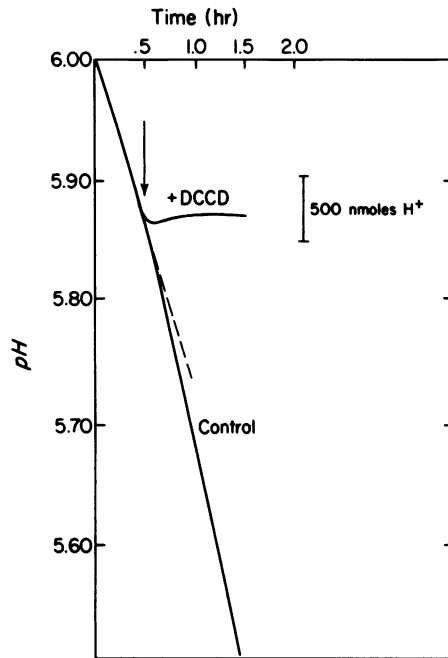


FIG. 3. The effect of DCCD on net H^+ efflux in continuous recording, illustrating the rapidity of the inhibitory action. Approximately 0.4 g fresh wt of roots in 100 ml of solution as in Table IV, 0.2 mM K° . 0.5% ethanol \pm DCCD added at arrow.

sum of these two components. The justification for this algebraic approach is given in the appendix. It is worthwhile to consider this separation in light of our previous suggestion that the K^+ -induced depolarization of ψ_p in the mechanism I range represents saturation of the K^+ carrier (11).

If we consider that ψ_p^I is nearly completely inhibited by DCCD, and that the remaining anoxia-sensitive potential is attributable

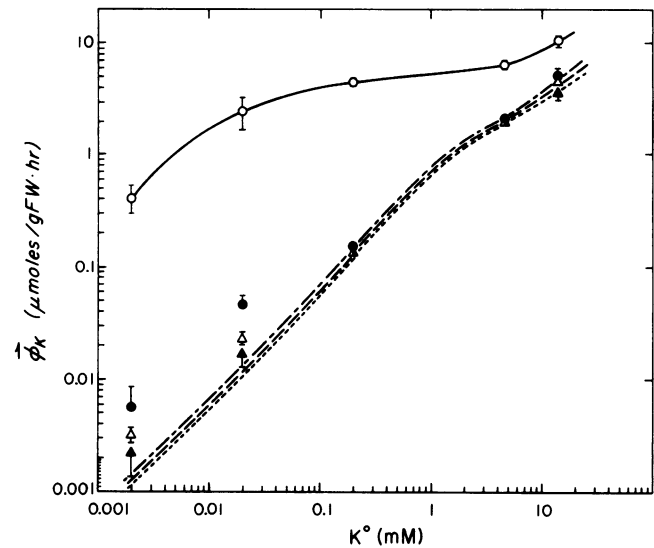


FIG. 4. K^+ (^{86}Rb) influx versus K° for control, and DCCD-pretreated tissue under aerobic and anoxic conditions. (○—○): Control; (Δ — Δ): anoxic; (●—●): +DCCD; (\blacktriangle — \blacktriangle): +DCCD and anoxic. Except for controls, lines were drawn from the η_K values in Table III, the ψ values based on Table I and ϕ_K predicted from equation 1. Note that a log-log presentation is used.

to ψ_p^{II} regardless of K° , we can also consider that active K^+ influx represents an ionic current shunted through the carrier rather than through passive channels. Figure 5 shows ψ_p redrawn from Figure 2 along with ψ_p^I and ψ_p^{II} as functions of K° . Note that we set ψ_p^{II} as having a constant minimum value of -17 mv in the mechanism I range; that is, DCCD inhibits only ψ_p^I , and there is a basal level of ψ_p^{II} detected in the mechanism I range in the presence of ATPase inhibition.

At 0.2 mM K° , K^+ influx is $>97\%$ active. It is thus justifiable to analyze mechanism I K^+ influx using the first order enzyme kinetic approach usually employed, without correction for passive influx. Kinetic analysis of the control data in Table III gives the apparent $K_m = 0.02$ mM and $V_{max} = 5.3$ $\mu\text{mol } K^+/\text{g fresh weight} \cdot \text{h}$. If carrier saturation depolarizes ψ_p^I we can compare per cent saturation with per cent reduction of ψ_p^I from its maximum values. The results (Table V) are consistent with the hypothesis that active K^+ influx depolarizes ψ_p^I .

The available evidence is consistent with the hypothesis that ψ_p^I arises from an electrogenic H^+/K^+ -ATPase in the plasmalemma (see Fig. 6 in ref. 12). The data in this paper indicate the ATPase is sensitive to DCCD, oligomycin, and DES (Table I). Balke and Hodges (4) have suggested that inhibition of an H^+/K^+ -ATPase accounts for the inhibition of K^+ influx. There is serious difficulty, however, in extending this concept to mecha-

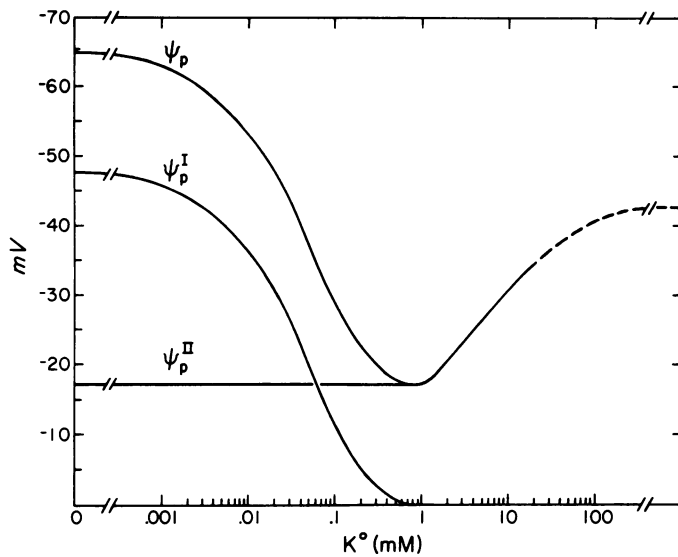


FIG. 5. The K° dependence of ψ_p and the hypothetical, additive components ψ_p^I and ψ_p^{II} . The further assumption has been made that ψ_p^{II} is constant in the low K° range at -17 mv.

Table V. Comparison of the Degree of Saturation of the Active K^+ Influx Mechanism with the Depolarization of ψ_p^I in the Low K° Range.

Maximum $\psi_p = -64$ mv; minimum ψ_p in controls = -17 mv. $\psi_p^{I,max} = -47$ mv.

| K° | $\phi_{\bar{K}}$ | ψ_p^I | $\phi_{\bar{K}}/V_{max}$ | $1 - \frac{\psi_p^I}{\psi_p^{I,max}}$ |
|-------------|---------------------------------|------------|--------------------------|---------------------------------------|
| mM | $\mu\text{mol/g}$ fresh wt·h | mv | | % |
| 0 | | -47 | | |
| 0.002 | 0.42 | -42 | 8 | 11 |
| 0.02 | 2.5 | -29 | 47 | 41 |
| 0.2 | 4.6 | -3 | 87 | 97 |

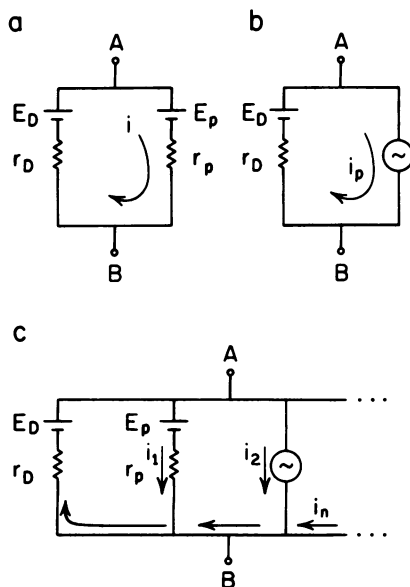


FIG. 6. Possible electrical analogues of the cell membrane containing one or more electrogenic systems. a: The electrogenic system as a voltage source; b: as a current source; c: multiple electrogenic systems. The restraint is included in c that current from one system can not be dissipated as negative current through another, other than the passive system.

nism II.

The data of Leonard and Hodges (27) for oat roots, of Leonard and Hotchkiss (28) for corn roots, and of Beggagna *et al.* (5) for corn coleoptiles and spinach leaves show a K^+ -stimulated (or more properly, a monovalent cation stimulated), DCCD-sensitive ATPase in isolated plasmalemma fractions which increases in activity up to 50 mM K^+ concentration. There is a strong correlation between the kinetics of K^+ influx and those of K^+ -stimulated ATPase activity over the 50 mM range (14, 26, 28). This suggests that a single ATPase is involved for both mechanism I and II. Bowman and Slayman (7) concluded that the plasmalemma of *Neurospora* contains a single ATPase. However, a single salt stimulated ATPase with a single mode of action is not consistent with the data obtained here and previously (12). To accommodate this we suggested that in the mechanism II range there is saturation and gradual suppression of the K^+ -carrying function of the ATPase, but with stimulation of ATPase activity and proton extrusion. With our present finding that ψ_p^{II} is not suppressed by the ATPase inhibitors (Figs. 2 and 5) even this modification must be reappraised. If a single ATPase is involved, its action at high K° must be inhibitor-insensitive.

A number of speculative mechanisms may be devised for ψ_p^{II} . Perhaps at high K° the ATPase shifts to pumping out K^+ or Na^+ rather than H^+ , and it is only the H^+ transport that is blocked by the ATPase inhibitors. The failure to detect an increase in net H^+ efflux between $K^{\circ} = 0.2$ and 4.6 mM (Table IV) might be interpreted in this way, as might the puzzling action of oligomycin (*e.g.* highly specific for the H^+ channel of the ATPase *in vivo*, but not effective when K^+ is extruded or in the isolated, salt saturated plasmalemma ATPase). Other possibilities are a DCCD-insensitive anion influx pump, or pumps that are linked to respiratory electron transfer. There is inadequate basis for pursuing any of these speculations.

Three points should be stressed. First, the effects of the ATPase inhibitors are not sufficiently understood to establish how they interfere with the electrogenic and K^+ influx systems. Existing studies with the isolated plasmalemma ATPase cannot be extrapolated to *in vivo* chemiosmotic models until it can be demonstrated that they pump protons and ions. Second, even if a single ATPase is involved in both functions, the functions are not obligatorily linked as shown by kinetic and electrophysiological studies. Binding of an inhibitor to one site (*e.g.* a proton channel) might not affect the action at another site of a complex enzyme. Third, regardless of the system(s) involved, all electrogenic parameters are dependent upon respiration. Thus the existence of an electrogenic, K^+ carrying, H^+ extruding ATPase which is inhibited by ATPase inhibitors and operates in the mechanism I range seems reasonable. However, no such assurance exists for the nature of mechanism II. It is in this range that passive K^+ influx dominates, that $\psi > E_K$, and the existence of an electrogenic potential (ψ_p^{II}) is established; the data cannot be explained by reasonable manipulation of the Goldman-Hodgkin-Katz equation for diffusion potentials (18). At this time it is not profitable to speculate on the biochemical-biophysical mechanisms involved. Analysis of existing models, however, may help clarify the electrical properties which must be explained. This is done for two widely used electrical models in the appendix.

LITERATURE CITED

- ANDERSON WP 1976 The electrophysiology of higher plant roots. In IF Wardlaw, JB Passioura, eds. Transport and Transfer Processes in Plants. Academic Press, New York pp 125-136
- BALKE NE, TK HODGES 1977. Inhibition of ion absorption in oat roots: comparison of diethylstilbestrol and oligomycin. Plant Sci Lett 10: 319-325
- BALKE NE, TK HODGES 1979 Effects of diethylstilbestrol on ion fluxes in oat roots. Plant Physiol 63: 42-47
- BALKE NE, TK HODGES 1979 Comparison of reductions in adenosine triphosphate content, plasma membrane-associated adenosine triphosphatase activity, and potassium absorption in roots by diethylstilbestrol. Plant Physiol 63: 53-56

5. BEFFAGNA N, S COCUCCHI, E MARRÈ 1977 Stimulating effect of fusicoccin on K-activated ATPase in plasmalemma preparations from higher plant tissue. *Plant Sci Lett* 8: 91-98
6. BOWMAN BJ, SE MAINSER, KE ALLEN, CW SLAYMAN 1978 Effects of inhibitors on the plasma membrane and mitochondrial adenosine triphosphatases of *Neurospora crassa*. *Biochim Biophys Acta* 512: 13-28
7. BOWMAN BJ, CW SLAYMAN 1979 The effects of vanadate on the plasma membrane ATPase of *Neurospora crassa*. *J Biol Chem* 254: 2928-2934
8. BYINGTON KH, JM SMOLY, AV MOREY, DE GREEN 1968 On the fragmentation of mitochondria by diethylstilbestrol. *Arch Biochem Biophys* 128: 762-773
9. CASEY RP, M THELAN, A AZZI 1979 Dicyclohexylcarbodiimide inhibits proton translocation by cytochrome *c* oxidase. *Biochem Biophys Res Commun* 87: 1044-1051
10. CHEESEMAN JM, JW GRONWALD, JB HANSON 1978 *In vivo* effects of DCCD on corn roots. *Plant Physiol* 61: S-29.
11. CHEESEMAN JM, JB HANSON 1979 Mathematical analysis of the dependence of cell potential on external potassium in corn roots. *Plant Physiol* 63: 1-4
12. CHEESEMAN JM, JB HANSON 1979 Energy-linked potassium influx as related to cell potential in corn roots. *Plant Physiol* 64: 842-845
13. CHEESEMAN JM, BG PICKARD 1977 Electrical characteristics of cells from leaves of *Lycopersicon*. *Can J Bot* 55: 497-510
14. FISHER JD, D HANSEN, TK HODGES 1970 Correlation between ion fluxes and ion-stimulated adenosine triphosphatase activity of plant roots. *Plant Physiol* 46: 812-814
15. GAUTHIER LM, JJ DIWAN 1979 Inhibition of K⁺ flux into rat liver mitochondria by dicyclohexylcarbodiimide. *Biochem Biophys Res Commun* 87: 1072-1079
16. GOLDSMITH TH, MHM GOLDSMITH 1978 The interpretation of intracellular measurements of membrane potential, resistance and coupling in cells of higher plants. *Planta* 143: 267-274
17. GRONWALD JW, JM CHEESEMAN, JB HANSON 1979 The response of fresh and washed corn roots to fusicoccin. *Plant Physiol* 63: 255-259
18. HIGINBOTHAM N 1973 Electropotentials of plant cells. *Annu Rev Plant Physiol* 24: 25-46
19. HODGES TK 1973 Ion absorption by plant roots. *Adv Agron* 25: 163-207.
20. HODGKIN AL 1951 The ionic basis of electrical activity in nerve and muscle. *Biol Rev* 26: 339-409
21. JACOBY B, OE PLESSNER 1970 Oligomycin effect on ion absorption by excised barley roots and their ATP content. *Planta* 90: 215-221
22. KAHN JS, JB HANSON 1957 The effect of calcium on potassium accumulation in corn and soybean roots. *Plant Physiol* 32: 312-316
23. KEIFER DW, RM SPANSWICK 1978 Activity of the electrogenic pump in *Chara corallina* as inferred from measurements of the membrane potential, conductance, and potassium permeability. *Plant Physiol* 62: 653-661
24. KITASATO H 1968 The influence of H⁺ on the membrane potential and ion fluxes of *Nitella*. *J Gen Physiol* 52: 60-87
25. KOZLOV IA, VP SKULACHEV 1977 H⁺-adenosine triphosphatase and membrane energy coupling. *Biochim Biophys Acta* 463: 29-89
26. LEIGH RA, RG WYN JONES 1975 Correlations between ion-stimulated adenosine triphosphatase activities and ion influxes in maize roots. *J Exp Bot* 26: 508-520
27. LEONARD RT, TK HODGES 1973 Characterization of plasma membrane associated adenosine triphosphatase activity of oat roots. *Plant Physiol* 52: 6-12
28. LEONARD RT, CW HOTCHKISS 1976 Cation-stimulated adenosine triphosphatase activity and cation transport in corn roots. *Plant Physiol* 58: 331-335
29. LIN W, JB HANSON 1974 Phosphate absorption rates and adenosine 5'-triphosphate concentrations in corn root tissue. *Plant Physiol* 54: 250-256
30. LIN W, JB HANSON 1976 Cell potentials, cell resistance, and proton fluxes in corn root tissue. Effect of dithioerythritol. *Plant Physiol* 58: 276-282
31. LÖPPERT H 1979 Evidence for electrogenic proton extrusion by subepidermal cells of *Lemma paucicostata* 6746. *Planta* 144: 311-315
32. MALONE CP, JJ BURKE, JB HANSON 1979 Histochemical evidence for the occurrence of oligomycin-sensitive plasmalemma ATPase in corn roots. *Plant Physiol* 60: 916-922
33. MARRÈ E 1977 Effects of fusicoccin and hormones on plant cell membrane activities: observations and hypotheses. In E Marrè, O Ciferri, eds, *Regulation of Cell Membrane Activities in Plants*. North Holland Publ Co, Amsterdam, pp 185-202
34. MARRÈ E, P LADO, F RASI-CALDOGNO, R COLOMBO, MI DE MICHELIS 1974 Evidence for the coupling of proton extrusion to K⁺ uptake in pea internode segments treated in fusicoccin or auxin. *Plant Sci Lett* 3: 365-379
35. PITMAN MG, WP ANDERSON, N SCHAEFER 1977 H⁺ ion transport in plant roots. In E Marrè, O Ciferri, eds, *Regulation of Cell Membrane Activities in Plants*. North Holland Publ Co, Amsterdam, pp 147-160
36. POOLE RJ 1978 Energy coupling for membrane transport. *Annu Rev Plant Physiol* 29: 437-460
37. PLONSEY R 1969 *Bioelectric Phenomena*. McGraw-Hill, New York
38. RYAN TE, CE BARR, JP ZORN 1978 Potassium transference in *Nitella*. *J Gen Physiol* 72: 203-218
39. SCHONER W, H SCHMIDT 1969 Inhibition of (Na⁺ + K⁺)-activated ATPase by N,N'-dicyclohexylcarbodiimide. *FEBS Lett* 5: 285-287
40. SPANSWICK RM 1972 Electrical coupling between cells of higher plants: a direct demonstration of intercellular communications. *Planta* 102: 215-227
41. SPANSWICK RM 1972 Evidence for an electrogenic ion pump in *Nitella translucens*. I. The effects of pH, K⁺, Na⁺, light and temperature on the membrane potential and resistance. *Biochim Biophys Acta* 288: 73-89

APPENDIX

ANALYSIS OF POSSIBLE ELECTRICAL ANALOGUES OF CELL MEMBRANES CONTAINING ELECTROGENIC SYSTEMS

The dependence of plant cell potential on the external ionic composition, and particularly on K⁺, is often more complex than expected from the Goldman-Hodgkin-Katz equation for the diffusion potential. In many plant cells the existence of an electrogenic system, probably in the plasmalemma, causing non-Goldman behavior is well established (18). Because of their locations, the passive and electrogenic systems are usually drawn to represent a parallel circuit. The extreme possibilities, as Keifer and Spanwick put it (23), are shown in Figure 6. These they have analyzed for their contributions to the electrical conductance of the membrane under an externally applied transmembrane current (23).

In the absence of this current, there can be no net transfer of charge across the cell membrane once ψ is established. Points A and B in Figure 6 are then points of reference for measuring the transmembrane voltage, V_{AB} (equivalent to the experimental parameter ψ). Analysis of these circuits to show the effects of varying the circuit parameters is a straightforward matter, yet well worthwhile; familiarity with the circuits allows more reasonable consideration of the implications of experimental results.

In Figure 6a, both batteries are directed the same; thus, in the loop circuit they "buck" each other. If $E_p \neq E_D$, current will flow through the loop. Any current through the pump side must also flow through the diffusion side, and the sum of all the voltage drops around the loop must be zero:

$$E_p - ir_p - ir_D - E_D = 0 \quad (A1)$$

(Note: since E_p and E_D are bucking, they have opposite signs in equation A1.) and

$$V_{AB} = E_p - ir_p = E_D + ir_D \quad (A2)$$

Modeling the pump as a current source (Fig. 6b) the restraint of zero net transmembrane current requires the pump current also flow through r_D , and

$$V_{AB} = E_D + i_p r_D \quad (A3)$$

Equations A2 and A3 are similar in form to that familiar in other reports (1, 24). However, it is clear from this analysis that the displacement of V_{AB} from E_D (or, experimentally, ψ from ψ_D) is due to the resistance of the passive channels (r_D) (see also ref. 1).

If either Figure 6, a or b is applicable, so long as the diffusion channels are not blocked in the presence of an electrogenic mechanism (*i.e.* $r_D \neq \infty$), the potential will be the algebraic sum indicated by equations A2 and A3. Furthermore, if more than one electrogenic system is included, and the further constraint is applied that the current carrying ion for each can not return via another electrogenic system (for example if a proton efflux pump, a sodium efflux pump, and a chloride influx pump all existed in one membrane) it is possible to consider the multisystem circuit shown in Figure 6c. Then the total current, i , which must flow through r_D is the sum of the individual pump currents,

$$i = i_1 + i_2 \dots + i_n \quad (A4)$$

and

$$V_{AB} = E_D + ir_D \quad (A5)$$

V_{AB} will change as E_D or any of the individual currents is changed. Our previous experimental convention has been to consider ψ_p as the algebraic difference between ψ and ψ_D (analogous to ir_D rather than to E_p). Equations A4 and A5 justify consideration of ψ_p as the sum of ψ_p^I and ψ_p^{II} .

The significant difference in behavior between the circuits in

Figure 6, a and b is the effect that alteration of parameters has on V_{AB} . In Figure 6a, the actual value of V_{AB} will be between E_D and E_p at a value determined by the ratio of the resistances. For simplicity let $r_p + r_D = 1$. Therefore,

$$i = \frac{E_p - E_D}{r_p + r_D} = E_p - E_D \tag{A6}$$

If $r_D \gg r_p$ (i.e. $r_D \rightarrow 1$), by equation A2 $V_{AB} = E_p$, and V_{AB} is totally insensitive to changes in E_D . If $r_p \rightarrow 1$, on the other hand, $V_{AB} = E_D$. If the ratio is not so extreme, an intermediate voltage will result. Then, changing E_p or E_D (for example, altering ψ_D by altering K°) will change V_{AB} by a lesser amount. For example, altering E_D ,

$$\Delta V_{AB} = \frac{r_p}{r_p + r_D} \Delta E_D \tag{A7}$$

Table VI relates this discussion to the observed K° dependence of ψ_p^{II} . Using the circuit of Figure 6a, let $E_p = -170$ mv, $r_p = 0.7$ and $r_D = 0.3$, all values constant. The apparent electrogenic component is $V_{AB} - E_D$. For comparison, values of K° , ψ_D , and ψ_p^{II} are included in the table. This exercise shows that no stimulation of an active process is required for the observed K° -de-

Table VI. Relationship of V_{AB} to E_D in the Voltage Source Model Circuit (Fig. 6a), Showing the Dependence of $V_{AB} - E_D$ on E_D

For the table, E_p , r_p , and r_D are constant at -170 mv, 0.7 , and 0.3 , respectively. For comparison to the biological case, corresponding values of K° , ψ_D , and ψ_p^{II} are given.

| E_D | $i = \frac{E_p - E_D}{r_p + r_D}$ | $V_{AB} - E_D = ir_D$ | K° | ψ_D | ψ_p^{II} |
|-------|-----------------------------------|-----------------------|-----------|----------|---------------|
| mv | | mv | mM | | mv |
| -99 | -71 | -21 | 0.002 | -99 | -17 |
| -98 | -72 | -22 | 0.02 | -98 | -17 |
| -97 | -73 | -22 | 0.2 | -97 | -17 |
| -91 | -79 | -24 | 0.86 | -91 | -17 |
| -71 | -99 | -30 | 4.6 | -71 | -27 |
| -49 | -121 | -36 | 13.8 | -49 | -33 |
| -32 | -138 | -41 | 29 | -32 | -37 |

pendent increase in ψ_p^{II} .

In the circuit of Figure 6b, if i_p and r_D are constant, it is clear from equation A3 that V_{AB} will be displaced from E_D by a constant value, regardless of alteration of E_D . Clearly, a current source can increase the electrogenic component ($V_{AB} - E_D$) only through an increase in pump activity. It is, of course, possible for both systems to occur, as shown in Figure 6c, and both characteristics will be maintained. Biologically, the current generator model is perhaps the more appropriate hypothesis for ψ_p^I where $\psi_D \approx$ constant. If ψ_p^I results from a pump current which can be "short circuited" by K^+ influx through the pump, the net i_p will be reduced as a result, producing the observations on saturation discussed in the main body of the paper.

Throughout this discussion we have considered the resistances to be constant. If the equilibrium conductance equation,

$$g = \frac{F^2}{RT} \phi \tag{A8}$$

applies to the passive channels (20) it is obvious that r_D is not constant, but decreases with increasing K° . As there has been no analysis which deals with passive conductance in nonequilibrium conditions or with membranes having significant electrogenic mechanisms, it is not certain how r_D behaves in tissue. The K° dependence of r_p is also unknown; so long as the relative magnitudes of r_D and r_p are constant, the analysis of Table VI is valid.

Spanswick (41) has suggested the circuit of Figure 6a applies in *Chara*, with $r_D \gg r_p$. Over a limited range, the cell potential does not respond when K° is increased (since the electrogenic mechanism shuts down abruptly above $K^\circ \approx 2$ mM (41), it is unclear exactly how much K° alters the diffusion potential to that point). This appears not to hold in higher plant roots as the potential responds throughout the K° range to changes in ψ_D . Finally note that it will not usually be possible even neglecting electrical coupling effects (13, 16, 40), to estimate E_p , in Figure 6a, by measuring resistance to an applied current. Using that technique, Ryan *et al.* (38) found the K^+ transference number in *Nitella* to be 0.83; i.e. 83% of the injected current is carried by K^+ through the membrane, yet the calculated passive K^+ conductance, (based on tracer flux in the absence of an applied current) was 20-fold too low to account for this. They concluded that the conductance equation (equation A8) normally used does not apply when a net current is passed across the membrane.